Available online at www.sciencedirect.com
ScienceDirect
ELSEVIER
Journal of Photochemistry and Photobiology A: Chemistry 182 (2006) 280–287
Journal of Photochemistry and Photobiology A:Chemistry
www.elsevier.com/locate/jphotochem

Continuous time random walk simulation of short-range electron transport in TiO_2 layers compared with transient surface photovoltage measurements

Ivan Mora-Seró [a,*], Juan A. Anta [b], Thomas Dittrich [c], Germà Garcia-Belmonte [a], Juan Bisquert [a,**]

[a] Departament de Ciències Experimentals, Universitat Jaume I, 12071 Castelló, Spain
[b] Área de Química Física, Universidad Pablo de Olavide, 41013 Sevilla, Spain
[c] Hahn-Meitner-Institute, Glienicker Str. 100, 14109 Berlin, Germany

Available online 5 June 2006

Abstract

The study of electron transport by transient surface photovoltage (SPV) measurements, in compact and nanoporous TiO_2 layers sensitized with dye at the outer surface, is summarized, extending previous results with continuous time random walk (CTRW) simulations in order to account for energy dispersion in the observed electron diffusion. In the case of nanoporous layers anomalous diffusion is observed immediately after electron injection for a wide temperature range, and the diffusion is consistent with an exponential distribution of traps that is affected by temperature variations. In the case of short-range diffusion in ultrathin compact TiO_2 layers, followed by electron recombination with the oxidized dye molecules, numerical simulation of electron transport with exponential distribution of traps with the CTRW approach provides an accurate description of the main features and time scales of the observed decays.
© 2006 Elsevier B.V. All rights reserved.

Keywords: Surface photovoltage; Spatial charge separation; TiO_2

1. Introduction

TiO_2 nanoparticle structures have received intense scrutiny due to the fact that this material has become very important for recent technological developments in broad fields: photovoltaics, photocatalysis, energy storage (batteries, supercapacitors), sensing, medicine and biophysics, catalysis, etc. The electron-transport dynamics in nanoporous electrodes plays a crucial role from both a fundamental science and device application perspectives. A large amount of research work has been developed in the study of diffusion, recombination and charge separation phenomena that determines the electronic processes in this material and its devices.

The surface photovoltage (SPV) technique is a contactless method [1] what makes it extremely attractive for the characterization of a wide spectrum of materials. One of the multiple variants of this technique studies the SPV time evolution after the sample was illuminated with a laser pulse, the so-called transient SPV. Time evolution of SPV allows investigating the carrier diffusion and recombination processes in the sample [1–6] as well as spatial charge separation process [7] in very short distances of the order of nm, and has the possibility to distinguish diffusion and recombination regimes even at very short timescales which are beyond the capabilities of the low frequency photoelectrochemical techniques. Regarding to a parallel plate capacitor configuration, a separation by only 1 nm of positive and negative charges with a density of 10^{12} cm^{-2} will already lead to a potential difference of the order of 5 mV which can be nicely measured by transient methods. This makes the SPV method interesting for charge separation even on molecular systems which do not have a space charge region.

The SPV transient of excess electron density injected in a layer, $\Delta n(x,t)$, is calculated from the double integration of the Poisson equation of the time dependent distribution:

$$\mathrm{SPV} = U(t) = \frac{e}{\varepsilon\varepsilon_0}\int_0^{L_S} \mathrm{d}x \int_0^{x} \Delta n(y,t)\,\mathrm{d}y \qquad (1)$$

* Corresponding author.
** Corresponding author. Tel.: +34 964728024 (O); fax: +34 964728066.
E-mail addresses: sero@exp.uji.es (I. Mora-Seró), bisquert@uji.es (J. Bisquert).

1010-6030/$ – see front matter © 2006 Elsevier B.V. All rights reserved.
doi:10.1016/j.jphotochem.2006.04.029

where e is the elementary charge, $\varepsilon_0 = 8.85 \times 10^{-14}\,\mathrm{F\,cm^{-1}}$ and ε is the dielectric constant. The SPV can provide direct information of charge separation due to the fact that it can be split up in two contributions: total amount of charge and distance between the centres of charge of the positive and negative carriers. It can be shown that [7]:

$$\mathrm{SPV}(t) = \frac{e}{\varepsilon\varepsilon_0} N(t)\langle x_n\rangle(t) \tag{2}$$

where $N(t)$ is the total amount of electrons (holes) per unit area at time t:

$$N(t) = \int_0^{L_\mathrm{S}} \Delta n(x,t)\,\mathrm{d}x \tag{3}$$

and $\langle x_n\rangle(t)$ is the mean position of electrons, i.e. their centre of charge:

$$\langle x_n\rangle(t) = \frac{1}{N(t)} \int_0^{L_\mathrm{S}} x\,\Delta n(x,t)\,\mathrm{d}x \tag{4}$$

In the more general case in which there are spatial distributions of both positive and negative charge carriers in the bulk, the separation formula adopts the form [7]:

$$\mathrm{SPV}(t) = \frac{e}{\varepsilon\varepsilon_0} N(t)(\langle x_n\rangle(t) - \langle x_p\rangle(t)) \tag{5}$$

$\langle x_p\rangle(t)$ is defined in the same way that in Eq. (4), but considering the excess distribution of holes, $\Delta p(x,t)$, instead of $\Delta n(x,t)$. $N(t)$ is the same for both distributions because recombination reduces identically positive and negative charge.

The direct interpretation of the time evolution of SPV in terms of the electronic processes is not straightforward and appropriate models are required to describe the experimental results. In the following sections we analyze the characteristics [5–7] of electron transport in nanoporous and compact TiO_2 layers, sensitized with N3 dye molecules in their outer surface, by transient surface photovoltage (SPV) measurements, with a view to extending the previous results [5–7] with more advanced models regarding the effect of traps on electron diffusion. First in Section 2, we discuss macroscopic diffusion in an assembly of TiO_2 nanoparticles and the observation of anomalous transport. It is also of great interest to investigate the electronic processes in the individual constituents of a network of interconnected nanoparticles, and to this end we have measured previously [5] SPV in ultrathin (few nanometer thick) TiO_2 layers as a model system to investigate the coupling of intra-particle transport with interfacial charge transfer. In Section 3, we present briefly the results of the observation of tunneling recombination of dye-photoinjected electrons at low temperature, and also an elementary model for electron diffusion and surface recombination along the layer [5]. While this model captures the main features of the experimental results, it has some important limitations. This is why we have developed a simulation method that takes into account both electron transport with trapping in the conditions of SPV measurement, and interfacial charge transfer. Numerical simulations based on CTRW approach, a method used previously for analyzing electron dynamics in dye-sensitized solar cells [8,9], are applied to SPV for the first time, and the results show a very realistic description of the measurements. The main conclusions and new research possibilities will be presented in the final section. We consider that these results can be taken as an example of the possibilities of SPV transients in the study of a broad range of mechanisms of charge injection, spatial charge separation, diffusion and recombination processes.

2. Long range diffusion in nanoporous TiO_2

A representative set of SPV transients at different temperatures for nanoporous TiO_2 sensitized with dye in the outer surface is shown in Fig. 1 [6]. The pulsed laser produces electronic excitation in the dye. Electrons are injected from the photoexcited dye into the TiO_2 layer leaving an uncompensated positive charge in the dye. This charge separation process may proceed within tens of fs during ultra-fast injection from dye molecules into TiO_2 and produces an initial distribution of electrons close to the surface and the starting SPV signal. Subsequently, electron diffusion increases the extent of charge separation and consequently the SPV signal.

For simplicity we consider the TiO_2 layer as an effective homogeneous medium with the outer surface positioned at $x = 0$ and the interface layer/substrate positioned at $x = L_\mathrm{S}$. In a first approximation we assume that the motion of electrons photoinjected in the TiO_2 layer follows the ordinary diffusion equation:

$$\frac{\partial \Delta n(x,t)}{\partial t} = D \frac{\partial^2 \Delta n(x,t)}{\partial x^2} \tag{6}$$

In the case of semi-infinite half-space and blocking boundary conditions at $x = 0$ the analytical solution of Eq. (6) is a semi-Gaussian:

$$\Delta n(x,t) = \frac{n_i}{\sqrt{\pi D t}} \exp\left(-\frac{x^2}{4Dt}\right) \tag{7}$$

The presence of additional shielding charges in the bulk of the porous TiO_2 film [10] may screen the electrical filed formed by the diffusing electrons. In a homogenous medium the screening length, λ_S, would be the Debye-screening length, λ_D:

$$\lambda_\mathrm{S} \approx \lambda_\mathrm{D} = \sqrt{\frac{\varepsilon\varepsilon_0 kT}{ne^2}} \tag{8}$$

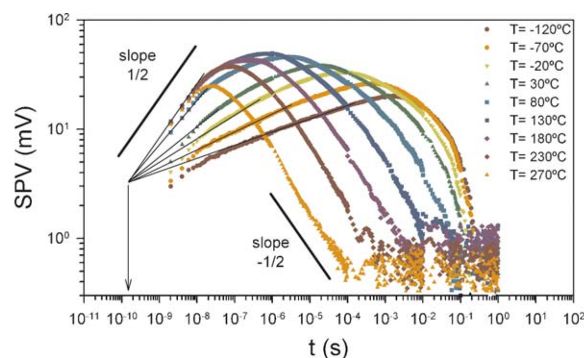

Fig. 1. Double logarithmic plots of SPV transients for different temperatures (intensities of the laser pulse $0.05\,\mathrm{mJ\,cm^{-2}}$). The laser pulse has been shifted to 16 ns. The arrow indicates the duration of the laser pulse, the straight lines approximate the power laws to this time.

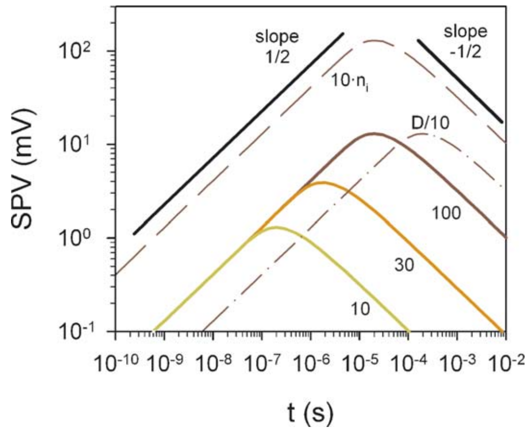

Fig. 2. SPV transients (log–log scale) obtained by Eq. (9), continuous lines takes into account a boundary for integration given by different λ_S values indicated near each curve in nm, considering $D = 10^{-6}\ cm^2\ s^{-1}$ and $n_i = 10^{14}\ cm^{-2}$. For a screening length of 100 nm the effect of changing D (dash-dot line) or n_i (dashed line), i.e. changing the incident light intensity, is also shown.

where k is the Boltzmann constant and T the temperature. Under the assumption of a screening length we consider that only the electron charge between $x = 0$ and $x = \lambda_S$ contributes to the SPV signal due to the screening of the charge diffusing away from $x = \lambda_S$. In this case the SPV can be calculated [6] as

$$\mathrm{SPV}(t) = \frac{2en_i}{\sqrt{\pi}\varepsilon\varepsilon_0}\sqrt{Dt}\left(1 - \exp\left(-\frac{\lambda_S^2}{4Dt}\right)\right) \qquad (9)$$

Fig. 2 shows some examples of calculated SPV transients ($n_i = 2 \times 10^{14}\ cm^{-2}$, $\varepsilon = 10$), using different values of λ_S, D and n_i. The amplitude of SPV depends linearly of λ_S. In all the cases the transients present a peak. The peak time of the SPV transient is proportional to the transit time, t_t (see the inset of Fig. 2, $t_{peak} \cong 2.5t_t$). t_t is defined as the time in which the width of the semi-Gaussian $\sigma = \sqrt{2Dt}$ attains a value $\sigma = \lambda_S$:

$$t_t = \frac{\lambda_S^2}{2D} \qquad (10)$$

Considering the relation (8), the dielectric relaxation time definition and the Einstein relation $D = kT\mu/e$ a simple relation $t_t = \tau_M/2$ is obtained. The peak time of the SPV transient is proportional to τ_M ($t_{peak} \cong 1.25\tau_M$). It is important to bring out that the dielectric relaxation time that is a bulk property can be obtained by SPV measurements that is a local technique, under the assumption (8).

Let us indicate the main predictions of the model. The evolution of SPV transients is better understood if we consider the total amount of electrons, $N(t)$, and the mean position of electrons $\langle x_n\rangle(t)$ in this case, given by [7]:

$$N(t) = n_i\,\mathrm{erf}\left(\frac{\lambda_S}{2\sqrt{Dt}}\right) \qquad (11)$$

$$\langle x_n\rangle(t) = \sqrt{\frac{4Dt}{\pi}}\frac{(1 - \exp(-\lambda_S^2/4Dt))}{\mathrm{erf}(\lambda_S/2\sqrt{Dt})} \qquad (12)$$

At short times $N(t)$ is constant and $\langle x_n\rangle(t)$ evolves with a power law with slope 1/2, as in the case of pure diffusion in a semi-infinite space, until for certain t_s, $\langle x_n\rangle(t)$ reaches a constant value $\langle x_n\rangle_{ct} = \lambda_S/2$. The apparition of this constant value of the charge separation is due to the finite nature of the region that contributes to the SPV. The SPV time dependence is only due to the charge separation and evolves with a power law with slope 1/2, see Fig. 2. t_s depends of the screening length and of the diffusion coefficient, and for $t > t_s$ the electron density $\Delta n(x,t)$ is practically uniform in the region between $0 \le x \le \lambda_S$ producing the saturation of the $\langle x_n\rangle(t)$ value to the half of the screening length of the sample. For long times the carriers diffuse away of the unshielded region $0 \le x \le \lambda_S$ and do not contribute anymore to the SPV. At these long times with $\langle x_n\rangle(t)$ constant the SPV time dependence is due to the reduction of charge that contributes to the SPV. The series expansion of $N(t)$, Eq. (11), predicts a power law with slope −1/2, and consequently, following Eq. (2), the SPV present the same time dependence, see Fig. 2. In summary the rise of the SPV is controlled by spatial separation $\langle x_n\rangle(t)$ and the decay by number of carriers $N(t)$. This analysis shows that Eq. (5) constitutes a useful tool to visualize and to study the time evolution of the spatial charge separation.

The previous model illustrates the effect of a shielding length on the SPV when the transient is governed by regular diffusion of electrons. The data in Fig. 1, however, show an additional trend that is not represented in that model. The SPV pattern follows a power law at low times with positive slope, α_i, which changes with temperature, and is smaller than 0.5 for temperatures different than the higher ones, indicating the occurrence of anomalous diffusion of electrons in the spatial range that is probed by SPV, $0 \le x \le \lambda_S$. It should also be noticed that the power law dependencies at the short times can be nicely approximated to a common intersection point at about 150 ps, i.e. the duration time of the laser pulse, see Fig. 1. The SPV at this point scales linearly with laser intensity [6] as predicted by the model, see Fig. 2 (t_{peak} does not scale linearly with laser intensity as expected, probably due to t_{peak} dependence on additional factors as dielectric relaxation, local screening and diffusion to a certain distance including in-homogeneities). Therefore, an initial distribution of excess electrons is formed within the duration of the laser pulse and anomalous diffusion of excess electrons can be observed immediately after switching off the laser pulse. At very long times and higher temperatures, the slope is practically independent of temperature and laser intensity, being about $\alpha_f = 0.5$, see Fig. 1. These observations indicate that the diffusion process is changing its character from anomalous diffusion at short times to normal diffusion at long decays.

Anomalous diffusion can be described with the fractional diffusion equation [11]. The mean square displacement is $r^2 \propto t^\alpha$ [12], where α, $0 < \alpha < 1$, is the dispersion parameter. A common way to explain the occurrence of anomalous diffusion in semiconductor materials is the presence of energy disorder in electronic states. In fact the CTRW model is related to the multiple trapping mechanism [13,14] in an exponential distribution of states. It has also been shown that a fractional diffusion equation is equivalent exactly to the CTRW formalism [15,16]. This equivalence holds when the *total charge* in traps is monitored [17], which is the case in SPV technique. We remark that calculations based on CTRW model have provided insight into the

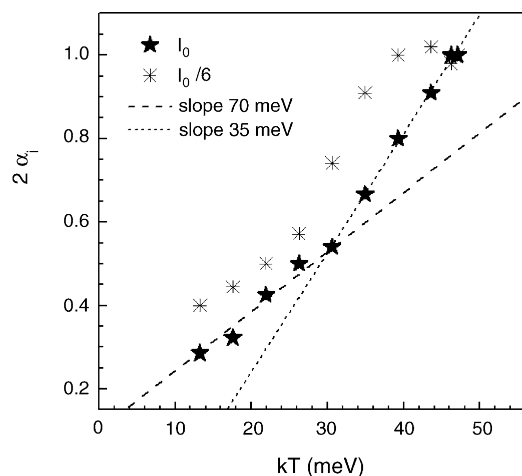

Fig. 3. Dependence of the power coefficient of anomalous diffusion (for the increasing parts of the SPV transients) on the thermal energy.

molecular mechanism of recombination dynamics in dye solar cells [18–20].

If the charge is conserved, the SPV is determined by the centre of charge, as discussed above in Eq. (2), and the voltage changes with time as $U \propto r \propto t^{\alpha/2}$. In this case the SPV transients will follow a power law with a power coefficient being half of the dispersion parameter of anomalous diffusion [6] instead of the coefficient 1/2 obtained for normal diffusion:

$$\mathrm{SPV}(t) \propto t^{\alpha/2} \tag{14}$$

In the case of a multiple trapping mechanism in an exponential distribution one has [21,22]:

$$\alpha = \frac{T}{T_0} \tag{13}$$

where T_0 is the parameter of the exponential distribution.

In Fig. 3, the values of $\alpha = 2\alpha_i$ are plotted as a function of kT. The increase of α with temperature is close to linear but a change of slope is observed, corresponding to a variation of the temperature parameter of the exponential distribution, T_0, from 800 to 400 K as the measurement temperature increases. It should be observed that one could expect changes of the distribution of states in the bandgap, as found recently in first-principle simulations of density of states (DOS) in TiO_2 quantum dots [23]. The change of the DOS is mainly an effect of the variation of the dielectric constant with temperature, which affects the energy of confinement of electrons in the quantum dots.

Therefore, while a single value of the exponential distribution does not describe all the results at different temperatures, it is found that energy disorder through the CTRW model constitutes a good first approximation to the experimental results.

3. Recombination and short-range diffusion in ultrathin TiO_2 layers

A representative set of SPV transients for several nm thick TiO_2 layers, sensitized with dye, at different temperatures is shown in Figs. 4 and 5 [5]. The signal remains stationary and

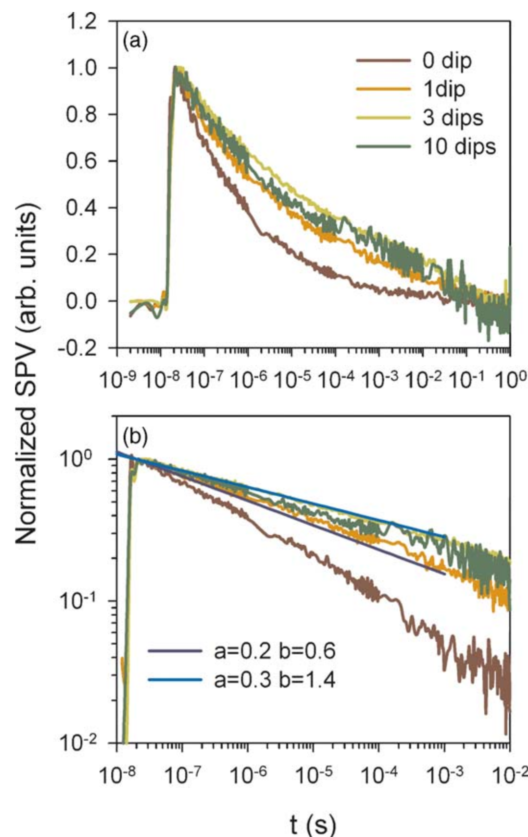

Fig. 4. Normalized photovoltage transients for TiO_2 compact layers with different thickness, 1–2 nm/dip, for low temperature ($T = -70\,^{\circ}$C). (a) Lin–Log scale. (b) Log–Log scale, theoretical results from Eq. (18), considering $\tau_0 = 2$ ps, for different a and b values in nm are also plotted.

decreases abruptly for high temperatures, Fig. 5, otherwise it may decrease from the first instant for low temperatures, Fig. 4. The SPV transient for low temperatures, Fig. 4, is independent of the film thickness. However at high temperatures, Fig. 5, as the layer thickness increases, the retardation of the SPV becomes much larger, providing the plateau region for the thickest sample. For reason of clarity we will analyze separately the results for low and high temperatures.

Since the low temperature results are independent of layer thickness, one may assume that the initial distribution of injected electrons remains stationary in space and decays only by tunneling recombination [2,24]. The rate R of recombination of electrons at a distance x from the surface is

$$R(x) = \frac{\Delta n}{\tau_0} e^{-2x/a} \tag{15}$$

where τ_0 is a phenomenological parameter, the lifetime for vanishingly small spatial separation, and a is the electrons Bohr radius. It has been determined in the study of SPV transients in nanoporous TiO_2 [6] that the value $\tau_0 = 2$ ps is the shortest possible time for back charge transfer of an electron into a charged dye molecule in TiO_2. The exponential distance dependence of the tunneling phenomenon should lead to an exponential distribution immediately after injection, considering that photoinjection of electrons from dyes into TiO_2 occurs also by tunneling [25]. The spatial distribution of excess electrons, $\Delta n(x,t)$, can be

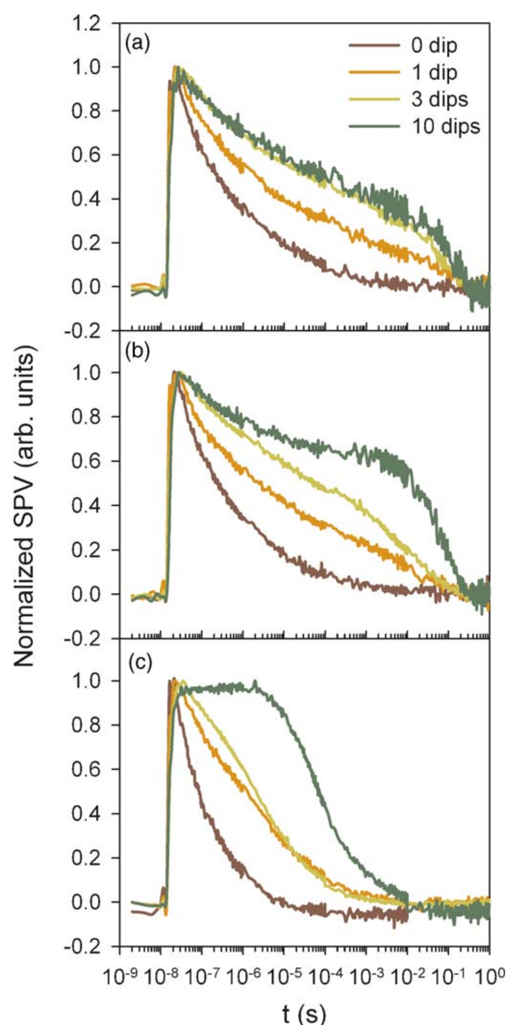

Fig. 5. Normalized photovoltage transients for TiO_2 compact layers with different thickness, 1–2 nm/dip, for higher temperatures than in Fig. 4. (a) $T = 30\,°C$; (b) $T = 80\,°C$; (c) $T = 230\,°C$.

obtained in the case of low temperatures from the equation:

$$\frac{\partial \Delta n}{\partial t} = -\frac{\Delta n}{\tau_0} e^{-2x/a} \tag{16}$$

which can be solved exactly and yields the time dependent electron distribution:

$$\Delta n(x, t) = n_0 \exp\left[-\frac{x}{b}\right] \exp\left[-\frac{t}{\tau_0} \exp\left(-\frac{2x}{a}\right)\right] \tag{17}$$

It was shown that for this distribution the SPV can be quite well approximated by the expression [5]:

$$U(t) = \frac{e n_0 a L_S}{2\varepsilon\varepsilon_0} \Gamma\left(\frac{a}{2b}\right)\left(\frac{t}{\tau_0}\right)^{-a/2b} \tag{18}$$

The photovoltage obeys a time dependent power law so that a straight line will be obtained in a log–log plot with a slope $-a/2b$. Fig. 4b shows the experimental value of SPV at low temperature for different layer thicknesses and the SPV transients calculated from the model of Eq. (18). It is found, averaging the slopes obtained for the three samples, that the ratio of electron Bohr

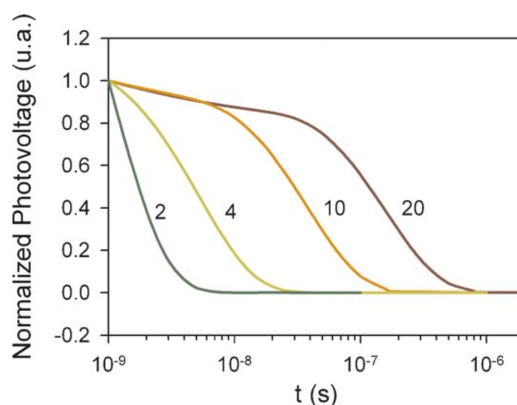

Fig. 6. Photovoltage transient simulations, normalized to the value of photovoltage at $t = 1$ ns, for various layer thickness indicated in nm, $D = 10^{-5}\,cm^2\,s^{-1}$, $\tau = 2$ ps, and $a = 0.25$ nm. The injected distribution at $t = 0$ is an exponential function with $\Delta n(x = 0) = 1 \times 10^{16}\,cm^{-3}$ and $b = 1$ nm.

radius and the exponential parameter in the initial distribution is $a/b = 0.28 \pm 0.04$. Most probable values obtained from this simulation of the experimental process are: a between 0.2 and 0.3 nm and b between 0.6 and 1.4 nm.

As the measurement temperature increases the SPV transients depart from the curve of decay at low temperature that is determined by recombination only (Fig. 5). This fact indicates that the electrons diffuse away from the injection region until they return also by diffusion to the high recombination region near the dye-covered surface, producing the fast decay observed at longer times. In zero-current measurement conditions, as in the case of transient SPV, the back contact behaves as a blocking interface limiting the extent of spatial charge separation. One expects that the larger the layer, the longer the PV remains high, and this is observed in the thickness dependence of the SPV transients at $T = 80$ and $230\,°C$, Fig. 5b and c.

In order to model the high temperature transients, the spatial distribution, $\Delta n(x,t)$, is obtained integrating the transport equation with tunneling recombination near the surface:

$$\frac{\partial \Delta n}{\partial t} = D\frac{\partial^2 \Delta n}{\partial x^2} - \frac{\Delta n}{\tau_0} e^{-2x/a} \tag{19}$$

Eq. (19) can be solved numerically allowing to calculate the SPV time evolution using Eq. (1) [5]. Fig. 6 shows simulated SPV transients for varying thickness of the film. The progressive retardation of the decay of the PV at increasing layer thickness due to longer diffusion time is clearly observed in the simulation as well as in the measurement in Fig. 4c and d. For the thinnest layer considered (2 nm), the charge separation by diffusion is strongly limited by the layer thickness producing a rapid SPV decay. For thicker samples the decay due to recombination is partially compensated by the spatial charge separation induced by diffusion. Charge separation increases progressively from low times until it attains a saturation value [7], as in the nanoporous layer, but in this case limited by the layer thickness instead of the screening length. The time at which the spatial charge separation attains its saturation coincides with the time position of the shoulder observed in the SPV transient, Fig. 6. After this time, the SPV signal exhibits a fast decay governed

by the back diffusion of electrons into the region of high recombination probability.

4. CTRW model simulations

The SPV patterns calculated from Eq. (19), can explain qualitatively the general trends observed in Fig. 4 but in the model simulation of Fig. 6 the SPV signal is observed to decay in a few time decades comparing with the experimental results which show the decay much more extended in time. This is not surprising since it is most likely that electron diffusion is strongly affected by the presence of traps, which tend to slow down considerable the rate of transport. In fact a wide variety of techniques have found that electron transport in nanoscale TiO_2 is well described with a model of energy disorder with an exponential trap distribution in the bandgap [9,26–28]. In particular, short-range electron dynamics into TiO_2 nanoparticles, preceding recombination of the electron with acceptor redox species, was described with CTRW formalism [19,20]. Also the SPV measurements discussed above, for the nanoporous TiO_2, indicate the presence of strong energy disorder.

For describing the decays of SPV in very thin films, it is mandatory to consider the highly inhomogeneous spatial electron distribution, which in combination with energy disorder, make it difficult to obtain an analytical solution for electron transport and surface recombination. Therefore we have applied the method of CTRW simulations of the time evolution of photoinjected electrons in the thin TiO_2 layer, used previously for analyzing electron dynamics in dye-sensitized solar cells [8,9], in order to obtain a more realistic description of the SPV transients in the ultrathin films.

In the previous sections we applied the one-dimensional diffusion equation to describe the SPV transients. In the following we study in detail the electrons random walk in a distribution of traps in the film. An electron in a site can hop in any direction, therefore we used a three-dimensional network of $n_x \times n_y \times n_z$ sites or *traps* with x being the direction perpendicular to the film surface. This direction is special concerning the recombination properties, as stated below in Eq. (22), therefore the simulation is still a one-dimensional model with symmetry in the y and z directions that neglects surface roughness and other similar geometric features. The number of sites in the x direction is fixed to correspond to the experimental film thickness. The lattice parameters is taken to be $a_L = 1$ Å. The optical depth utilized was $b = 0.5$ nm and the electrons Bohr radius $a = 0.5$ nm. The number of sites in the y and z directions is selected so that the system reproduces the experimental surface electron density.

The energies of the traps are taken from an exponential distribution defined by

$$g(E) = \frac{N_t}{kT_0} \exp\left(\frac{E}{kT_0}\right) \tag{20}$$

where E is the energy separation of the trap with respect to the conduction band (definite positive). Thus, *deep* traps correspond to large E-values and *shallow* traps to small values of E. Large values of T_0 imply a trap distribution with a large proportion of deep traps. Each trap i is given a release time according to

$$t_i = -\ln(r) t_0 \exp\left(\frac{E_i}{kT}\right) \tag{21}$$

where r is a random number uniformly distributed between 0 and 1 and t_0 is the inverse of the so-called attempt-to-jump frequency. In these calculations t_0 is an adjustable parameter. Analogously, each trap i is given a recombination time extracted from

$$t_i^{\mathrm{R}} = -\ln(r) t_0^{\mathrm{R}} \exp\left(\frac{2x}{a}\right) \tag{22}$$

The recombination times are scaled by t_0^{R}, which acts as an adjustable parameter. This corresponds to the recombination time of an electron for vanishingly small spatial separation. Eq. (22) is introduced to reproduce removal of electrons from the sample by tunneling recombination as described above.

The calculation is carried on by running a number of simulations for different realizations or samples of the distribution (20) for the network of traps. The final result is averaged over the total number of samples utilized. For each simulation a certain number of electrons are injected into the sample with a probability proportional to $\exp(-x/b)$, where x is the distance to the film surface. As indicated in Ref. [8], electrons are moved according to the release times specified by Eq. (21). During the simulation the electrons adopt the release times and the recombination times of the sites that they visit. For each simulation the electron with the shortest release time ($t_{\min}$) is moved to a neighbouring site chosen at random. This time is then used to advance the total simulation time and to reduce accordingly the release and recombination times of the rest of the electrons. If the recombination time of a certain electron exceeds $t_{\min}$, this electron is removed from the sample. The simulation is finished when all the electrons in the box run out. During the simulation both the injecting and the opposite surface acts as blocking contacts. Periodic boundary conditions are applied along the y and z directions. The electron density as a function of x and time was extracted from a histogram in which the position of the electrons is recorded for specific time intervals distributed logarithmically. The SPV is then obtained employing Eq. (1).

Most of the simulations were carried out using 4 electrons and 200×200 sites in the y and z directions. In this case the surface density is $4/(200 \times 200 \times 1\,\text{Å}^2) = 1.00 \times 10^{16}\,\text{m}^{-2}$. It has been observed that using more electrons with the same surface density (for instance 10 electrons and 300×300 sites give equivalent results). The number of numerical samples utilized ranged between 100 and 5000. More samples are needed to obtain "smooth" curves although a few samples are sufficient to see the trend in the photovoltage decays.

In order to cover most of the cases studied in the experiments [5] we considered three temperatures, 200, 300 and 500 K, and two film thickness, 2 and 20 nm, corresponding to 20 and 200 sites on the x-direction, respectively. As for the characteristic recombination time t_0^{R}, it has been observed that the choice that leads to a better accord with the experiments is $t_0^{\mathrm{R}} = 50 t_0$.

We can distinguish two regimes for the calculated photovoltage decays:

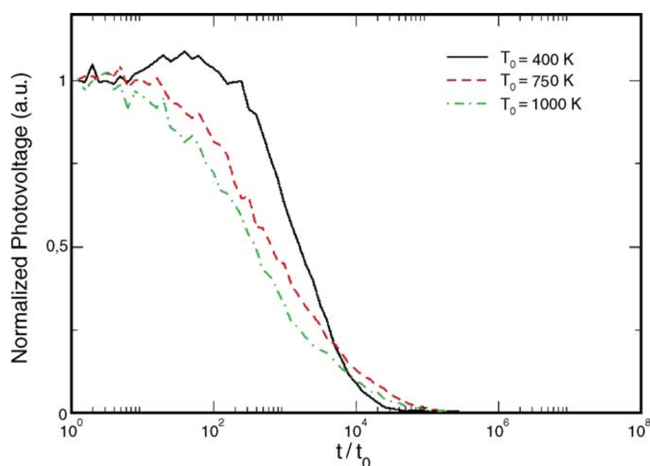

Fig. 7. Normalized surface photopotential as extracted from continuous time random walk simulations for ultrathin TiO_2 samples considering that the energies of the traps are exponentially distributed. Three different characteristic temperatures were considered in this graph. All calculations were carried for $T = 300$ K, $d = 2$ nm and using $t_0^R = 50t_0$.

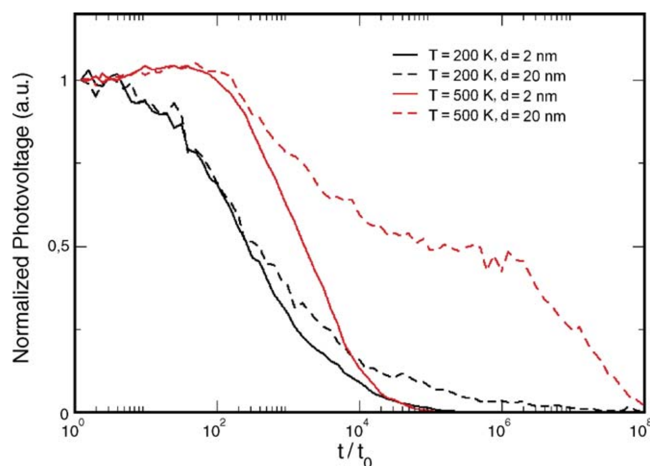

Fig. 8. Same as Fig. 7 but now showing the effect of ambient temperature and film thickness. A single exponential distribution with characteristic temperature 750 K was utilized in all cases.

(1) The photovoltage is controlled by tunneling recombination. This predominates at lower temperatures (or deep trap distributions) and the characteristic shape is an exponential-like decay.
(2) The photovoltage is controlled first by diffusion and then by recombination. This predominates at larger temperatures (or shallow trap distributions) and the characteristic shape is a slowly decaying "plateau" followed by a rapid decrease.

When the photovoltage is controlled by tunneling the decay is observed to be independent of the film thickness, as observed experimentally for low temperatures. When the photovoltage is controlled by diffusion the "plateau" reaches longer times for thicker samples.

Three different trap distributions corresponding to $T_0 = 400$, 750 and 1000 K have been analyzed (see Fig. 7). The first of them corresponds to a situation with very shallow traps. The result is that the photovoltage exhibits very long "plateaus". On the contrary, for $T_0 = 750$ and 1000 K the photovoltage is controlled by diffusion only at high temperatures. The traps are now deeper and this makes the electrons to stay longer in sites close to the injecting surface (for which the recombination times are shorter).

The CTRW method reproduces the basic observations of the experiments. An exponential trap distribution with $T_0 = 750$ K seems to be the one that reproduces more faithfully the observations found in the SPV measurements, as shown in Fig. 8. Importantly, in the temperature range where diffusion is active, the simulation shows a two-step decay, first with a low and then with a high slope, as in the measurements shown in Fig. 5. Furthermore the SPV decay is extended over several decades in time, in contrast with the simpler model without traps discussed above.

These results of CTRW simulation are encouraging towards a complete description of electron transport and recombination in ultrathin layers by means of energy disorder. However, it was not possible to find an unique exponential trap distribution that is capable to explain the experimental results for all temperatures and film thicknesses. In this context the use of trap distributions different from the exponential function [8] or affected by temperature variation might be a good choice to fit more realistically the experimental observations. Additionally a degree of structural disorder [29], not considered in the model, may affect the recorded data. The thicker compact samples analyzed in this study consist of anatase and amorphous phases after annealing at 400 °C, as it has been checked by Raman spectroscopy, and the thinner layers present a considerable roughness indicating a poor layer thickness uniformity, and trap distribution may vary with layer thickness.

5. Conclusions

The transient SPV technique has allowed us to observe anomalous diffusion, in the case of nanoporous TiO_2 layers, for a wide temperature range, taking into account that the SPV is locally limited to the region where charge separation takes place, i.e. to a near surface layer with a thickness of the screening length. In the case of ultrathin samples diffusion and tunneling recombination have been observed. At low temperatures (100–250 K) the dynamics is governed exclusively by spatially dependent tunneling recombination. For high temperatures (250–540 K), the dynamics of surface recombination is retarded by the diffusion of electrons towards the interior of the film. The CTRW method based on energy disorder with an exponential distribution describes detailed features of the decays, as well as their extended time scales, but does not explain with a single exponential trap distribution the decays observed in all cases.

Acknowledgements

The work was supported by Ministerio de Educación y Ciencia of Spain under project MAT2004-05168 and Acción Integrada UJI-HMI. JAA also thanks Ministerio de Educación y Ciencia of Spain for support under grant ENE2004-01657/ALT.

References

[1] L. Kronik, Y. Shapira, Surf. Sci. Rep. 37 (1999) 1.
[2] T. Dittrich, V. Duzhko, F. Koch, V. Kytin, J. Rappich, Phys. Rev. B 65 (2002) 155319.
[3] V. Duzhko, F. Koch, T. Dittrich, J. Appl. Phys. 91 (2002) 9432.
[4] V.Y. Timoshenko, V. Duzhko, T. Dittrich, Phys. Stat. Sol. (a) 182 (2000) 227.
[5] I. Mora-Seró, T. Dittrich, A. Belaidi, G. Garcia-Belmonte, J. Bisquert, J. Phys. Chem. B 109 (2005) 8035.
[6] T. Dittrich, I. Mora-Seró, G. Garcia-Belmonte, J. Bisquert, Phys. Rev. B 73 (2006) 045407.
[7] I. Mora-Seró, T. Dittrich, G. Garcia-Belmonte, J. Bisquert, submitted for publication.
[8] J.A. Anta, J. Nelson, N. Quirke, Phys. Rev. B 65 (2002) 125324.
[9] J. Nelson, Phys. Rev. B 59 (1999) 15374.
[10] V. Kytin, T. Dittrich, J. Bisquert, E.A. Lebedev, F. Koch, Phys. Rev. B 68 (2003) 195308.
[11] R. Metzler, J. Klafter, Phys. Rep. 339 (2000) 1.
[12] R. Metzler, E. Barkai, J. Klafter, Phys. Rev. Lett. 82 (1999) 3563.
[13] F.W. Schmidlin, Phys. Rev. B 16 (1977) 2362.
[14] G. Pfister, H. Scher, Adv. Phys. 27 (1978) 747.
[15] R. Hilfer, J. Phys. Chem. B 104 (2000) 3914.
[16] R. Hilfer, in: R. Kutner, A. Pekalski, K. Sznaij-Weron (Eds.), Anomalous Diffusion—From Basics to Applications, Springer, Berlin, 1999, p. 77.
[17] J. Bisquert, Phys. Rev. Lett. 91 (2003) 010602.
[18] J. Nelson, S.A. Haque, D.R. Klug, J.R. Durrant, Phys. Rev. B 63 (2001) 205321.
[19] A.V. Barzykin, M. Tachiya, J. Phys. Chem. B 106 (2002) 4356.
[20] A.V. Barzykin, M. Tachiya, J. Phys. Chem. B 108 (2004) 8385.
[21] J. Orenstein, M. Kastner, Phys. Rev. Lett. 46 (1981) 1421.
[22] T. Tiedje, A. Rose, Solid State Commun. 37 (1981) 49.
[23] J.L. Movilla, G. Garcia-Belmonte, J. Bisquert, J. Planelles, Phys. Rev. B 72 (2005) 153313.
[24] H.J. Queisser, D.E. Theodorou, Phys. Rev. B 33 (1986) 4027.
[25] M. Tachiya, A. Mozuber, Chem. Phys. Lett. 34 (1975) 77.
[26] J. van de Lagemaat, A.J. Frank, J. Phys. Chem. B 104 (2000) 4292.
[27] J. van de Lagemaat, N. Kopidakis, N.R. Neale, A.J. Frank, Phys. Rev. B 71 (2005) 035304.
[28] M. Bailes, P.J. Cameron, K. Lobato, L.M. Peter, J. Phys. Chem. B 109 (2005) 15429.
[29] N. Kopidakis, J. van de Lagemaat, K.D. Benkstein, A.J. Frank, Q. Yuan, E.A. Schiff, Phys. Rev. B 73 (2005) 045326.